Synchrotron x-ray photoemission study of soft x-ray processed ultrathin glycine-water ice films

George Tzvetkov[1,a] and Falko P. Netzer[2]
[1]*Department of Inorganic Chemistry, Faculty of Chemistry, University of Sofia, James Bourchier 1, 1164 Sofia, Bulgaria*
[2]*Institut für Physik, Oberflächen- und Grenzflächenphysik, Karl-Franzens Universität Graz, A-8010 Graz, Austria*

(Received 18 March 2011; accepted 27 April 2011; published online 26 May 2011)

Ultrathin glycine-water ice films have been prepared in ultrahigh vacuum by condensation of H_2O and glycine at 90 K on single crystalline alumina surfaces and processed by soft x-ray (610 eV) exposure for up to 60 min. The physicochemical changes in the films were monitored using synchrotron x-ray photoemission spectroscopy. Two films with different amounts of H_2O have been considered in order to evaluate the influence of the water ice content on the radiation-induced effects. The analysis of C1s, N1s, and O1s spectral regions together with the changes in the valence band spectra indicates that amino acid degradation occurs fast mainly *via* decarboxylation and deamination of pristine molecules. Enrichment of the x-ray exposed surfaces with fragments with carbon atoms without strong electronegative substituents (C–C and C–H) is documented as well. In the thinner glycine-water ice film (six layers of glycine + six layers of water) the 3D ice suffers strongly from the x-rays and is largely removed from the sample. The rate of photodecomposition of glycine in this film is about 30% higher than for glycine in the thicker film (6 layers of glycine + 60 layers of water). The photoemission results suggest that the destruction of amino acid molecules is caused by the direct interaction with the radiation and that no chemical attack of glycine by the species released by water radiolysis is detected. © *2011 American Institute of Physics*. [doi:10.1063/1.3591337]

I. INTRODUCTION

The radiation-induced chemistry of organic molecules in condensed water has attracted much attention recently.[1–5] The understanding of these processes is of importance in various fields including astrochemistry,[6,7] atmospheric chemistry,[8] and radiobiology.[9] Among the organic/water systems, low temperature water films containing amino acids, i.e., the simplest biologically active molecules and building blocks of proteins, are of particular interest. The effects of radiative processing of the latter systems are of significance in prebiotic organic chemistry, specifically the creation of amino acid molecules in the interstellar space and their delivery to our planet. Recently, several amino acids have been synthesized by UV irradiation of interstellar ice analogs containing H_2O, CH_3OH, NH_3, CO, and CO_2.[10] Furthermore, glycine (the simplest amino acid) has been conclusively detected in the material ejected from comets.[11,12] Thus, the resistance of amino acids–water ice systems to the energetic radiation through their transfer from space to Earth is a fundamental question for the origin and the early evolution of life on our planet.

In the past decades, many radiation effects in condensed water have been identified in the laboratory experiments. In summary, excitations promoted by visible, UV, and soft x-ray photons and low energy electrons (0–600 eV) induce dissociation, desorption, and structural transformations in thin water films.[13] These processes are mainly due to the inelastically scattered electrons. When the sample is irradiated with photons, these electrons are created in photoionization and subsequent inelastic scattering events. The chemical changes in thin films and fine powders of amino acids under the impact of electrons and photons have also been investigated. For instance, it was found that soft x-ray irradiation of several amino acids under ultrahigh vacuum (UHV) conditions leads to a decomposition of the molecules *via* several pathways, including dehydrogenation, decarboxylation, deamination, and dehydration.[14–20] So far, little is known on the radiation-induced processes in mixed glycine-water ice films. Only very recently, Lattelais *et al.*[21] reported on the effect of soft x-ray irradiation of glycine diluted into water ice at 30 K. On the basis of the x-ray absorption spectroscopy examinations, it was found that water neither protects nor enhances the glycine photodecomposition.

In the present work, the physicochemical transformations in mixed glycine-water ice ultrathin layers upon prolonged soft x-ray illumination were studied by means of synchrotron x-ray photoemission spectroscopy. Three-dimensional glycine-water ice films with different architecture have been grown under controlled UHV conditions by co-deposition on a single crystalline aluminum oxide substrate surface. The samples were illuminated with high-brilliance 610 eV x-rays for 60 min and subsequently analyzed. This study extends the quite limited knowledge of the interactions of x-rays with mixed amino acids-water ice systems. Moreover, the information obtained is of general importance for future investigations of organic and bioorganic systems with ionizing beams, where radiation induced changes can occur.

[a]Author to whom correspondence should be addressed. Electronic mail: nhgtz@wmail.chem.uni-sofia.bg. Telephone: +3592-8161-206. Fax: +3592-9625-438.

II. EXPERIMENT

The experiments were performed in two UHV systems (base pressure $<2 \times 10^{-10}$ mbar) equipped with standard surface preparation and different analytical tools. The photoemission measurements were performed at the UE52-PGM undulator beamline at the BESSY II storage ring in Berlin with a Scienta SES200 hemispherical energy analyzer. The photon beam was incident at 55° relative to the surface normal, and the spectra were recorded at normal emission. Photon energy of 610 eV was used for exciting electrons from the C1s, N1s, and O1s core levels, respectively. Additional valence band photoemission measurements were performed at photon energy of 160 eV. The combined monochromator-analyser energy resolution was better than 110 meV ($h\nu = 160$ eV) and 140 meV ($h\nu = 610$ eV) as determined from the widths of the Fermi edges measured on a clean NiAl(110) crystal. The fitting of the core level spectra was performed by using mixed Gaussian/Lorenzian peak shapes. To compensate for charging effects, the binding energy (BE) scale was adjusted to provide a BE of 289.8 eV for the C1s component corresponding to carbon from the carboxyl group (–COOH). All spectra were normalized to the maximum intensity. The structure of the starting glycine-water ice layers was evaluated by means of temperature-programmed desorption (TPD). TPD experiments were carried out in a custom-designed μ-metal chamber with a line-of-sight detection quadrupole mass spectrometer, which is surrounded by a liquid nitrogen cooled stainless steel shield in order to suppress the detection of gases desorbing from the crystal holder and chamber walls.[22] Spectra were collected at a linear heating rate of 1 K/s generated with a homebuilt computer controlled power supply. In both chambers the temperature of the sample was monitored by a K-type (chromel–alumel) thermocouple attached to the backside of the NiAl(110) crystal.

Single crystalline alumina AlO_x film surfaces have been prepared as substrates by thermal oxidation of a NiAl(110) single crystal surface followed by high temperature annealing, as described in the literature.[23] This ultrathin alumina film was chosen as a substrate for two reasons: first, because of its inertness toward adsorbed adlayers (the AlO_x film is oxygen terminated)[24], and second, because of the previously obtained data about the properties of glycine and water adsorbates on this surface.[25–27]

Vapor deposition of glycine (NH_2CH_2COOH) was achieved from a specially designed Knudsen cell-type molecule evaporator. The glycine powder (>99%, Fluka) was introduced into a small copper cell heated by a button heater attached to its backside. This evaporation source was separated from the UHV chambers by a gate valve and pumped by a turbomolecular pump. Before evaporation, the glycine was carefully outgassed for several hours at 370 K with the gate valve closed. During deposition, the evaporator was moved toward the sample surface, and the glycine powder was kept at 400 K. The mixed glycine-ice layers were prepared by depositing glycine on to the alumina surface at 90 K (110 K for TPD measurements) in a H_2O background pressure (up to $\sim 10^{-7}$ mbar). High-purity water (H_2O, puriss. p.a. grade) was obtained from Fluka, and was further purified by several freeze–pump–thaw cycles. Because of the slow pumping rate of the water after background dosing in the system in Berlin, the values associated with the XPS spectra may slightly underestimate the real exposure. The radiation-induced changes in the condensed glycine-water ice films were stimulated during the normal core shell photoemission experiments. The spectra were taken repeatedly at the same position on the sample, starting with C1s region and followed by N1s and O1s spectral regions. The maximum exposure time was 60 min and the size of the beam spot on the sample was approximately 0.8×0.2 mm^2. At the mean storage ring current of 100 mA, the photon flux is estimated to be 3×10^{11} photons/s.

III. RESULTS

A. Structure of the as-grown glycine-water ice films

Two films with different architecture have been examined in our study in order to evaluate the influence of the water ice content on the beam-induced effects. They have been prepared by co-deposition of 6 layers of glycine (determined from the desorption peak areas in TPD and referenced to the saturated first monolayer of glycine on AlO_x)[27] and 10 layers of water (structure denoted as G6W10) and, respectively, co-deposition of 6 layers of glycine and 60 layers of water (structure denoted as G6W60) onto the AlO_x alumina surface. One layer of ice is defined here as the saturation layer of H_2O on AlO_x at 110 K. On the basis of our previous studies, we estimate that one layer corresponds to $\approx 5.9 \times 10^{14}$ molecules/cm^2.[22] When deposited at temperatures 90–130 K under vacuum, water vapors condense in the so-called low-density amorphous (LDA) ice.[28,29] The morphology of this phase depends on the nature of the substrate,[30] the temperature, and the angular distribution of the incident water molecules.[31,32] According to Stevenson *et al.*,[32] amorphous water films grown from ambient vapors above ~90 K are uniform with a density very similar to that of the crystalline ice grown at 145 K.

TPD spectra from G6W10 and G6W60 films are presented in Fig. 1. Figure 1(a) displays the desorption curves of H_2O (atomic mass unit 18) and Fig. 1(b) shows the desorption curves of glycine (atomic mass unit 30, which is the most intense peak of the mass spectrometric fragmentation pattern of glycine corresponding to $CH_2NH_2^+$). H_2O TPD curves of 10 and 60 layers of pure water as well as the TPD curve of 6 layers of glycine deposited onto AlO_x are also displayed. As one can see, there is no detectible temperature shift or changes in the lineshapes of the TPD traces of glycine from G6W10 and G6W60 films in comparison to the spectrum of pure glycine. Furthermore, there are no changes in the H_2O TPD curve from G6W10. The leading edges of the two curves have a characteristic shoulder at the onset of desorption at 150–160 K, which has been associated with the amorphous-to-crystalline phase transition of the LDA ice.[33] This is a strong indication that glycine molecules do not interact with water during codeposition and subsequent heating of the G6W10 film. In contrast, the H_2O TPD curve from G6W60 differs significantly from the curve of pure water ice. Namely, there is a shift

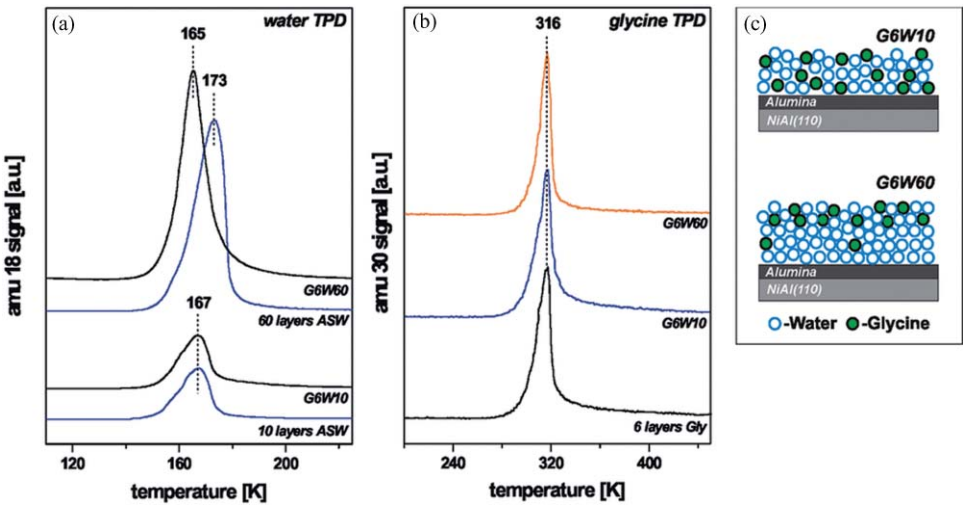

FIG. 1. Temperature-programmed desorption spectra of (a) H_2O and (b) glycine from 6 layers of glycine intermixed with 10 layers of water ice (G6W10) and 6 layers of glycine intermixed with 60 layers of water ice (G6W60) on alumina. The spectra from 10 and 60 layers of water ice as well as from 6 layers of glycine adsorbed on alumina are also presented. (c) A schematic representation of the G6W10 and G6W60 films organization (structures not to scale).

of the TPD curve maximum by 8 K toward lower temperature and a lack of the shoulder at the onset of desorption (see Fig. 1(a)). We have shown in our previous studies that the intermixing of 50 layers of water ice and 4 layers of glycine on the same substrate leads to the same shift in the corresponding H_2O TPD signal.[26] This effect has been ascribed to the suppression of the amorphous-to-crystalline phase transition of LDA by the embedded glycine molecules and subsequent desorption of H_2O from an amorphous-like situation. Furthermore, on the basis of the N1s and O1s angle-resolved photoemission spectroscopy analysis of the mixed films, this effect is accompanied by the phase separation between H_2O and glycine, where the glycine phase accumulates near the surface of the films, displaying a hydrophobic behavior.[22,26]

Thus, the mixed glycine-water ice films subjected to soft x-ray irradiation possess different architecture. In the G6W10 film, glycine and water molecules are homogeneously intermixed. When the same amount of glycine is suspended in the thicker water ice film (G6W60), glycine and water molecules form separate phases with little intermixing and with the glycine molecules located predominantly at the vacuum-solid interface. The structural models of G6W10 and G6W60 films are sketched in Fig. 1(c).

B. Radiation-induced effects in the G6W10 film

The time evolution of the C1s photoemission spectrum of G6W10 film upon exposure to 610 eV x-rays is shown in Fig. 2(a). The peak-fitting results of the spectra from the pristine film and after 20, 40, and 60 min of irradiation are included in the same figure. The photoemission spectrum of the as-grown G6W10 film shows two main components at 287.7 and 289.8 eV and a very weak component at 285.8 eV. The component at 287.7 eV corresponds to the aliphatic carbon (CH_2NH_2) in the glycine molecule; the component at ~290 eV is assigned to the carbon from the carboxyl group (–COOH). The binding energies (BEs) and energy separation of these two components (2.1 eV) agree well with the previously reported data for the zwitterionic glycine in the solid state ($NH_3{}^+CH_2COO^-$).[34,35] The integrated intensity ratio of the C1s components ($CH_2NH_2/COO^- = 0.96$) for glycine in the pristine G6W10 film is in good agreement with the molecular stoichiometry. Figure 2(b) shows the integrated intensity ratio of these two components as a function of irradiation time. The continuous increase of the ratio indicates the beam-induced reduction of the carboxyl carbon fraction in G6W10.

Based on the results of previous XPS studies of solid glycine, we ascribe the component at 285.8 eV to hydrocarbon fragments resulting from glycine decomposition due to the x-ray illumination.[20,35] After 40 min of irradiation an additional small component in the C1s spectrum at 284.6 eV is resolved in Fig. 2(a). According to the BE position of this peak, we presume that it is due to the C–C bonded graphitic-type of carbon formed as a result of the prolonged illumination. As shown in Fig. 2(a), both low BE spectral features

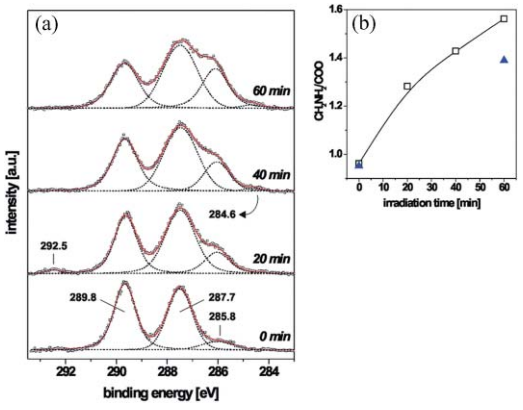

FIG. 2. (a) Time evolution of C1s photoemission spectrum of G6W10 during continuous exposure to x-rays; spectra at the beginning of irradiation (0 min) and after 20, 40, and 60 min are presented. The dots are the measured data points, and the dashed lines are the components determined by the fitting procedure. The solid lines through the data points are the results of the fitting. (b) CH_2NH_2/COO^- integrated intensity ratio for G6W10 (open symbols) and for G6W60 (filled symbols) as a function of irradiation time.

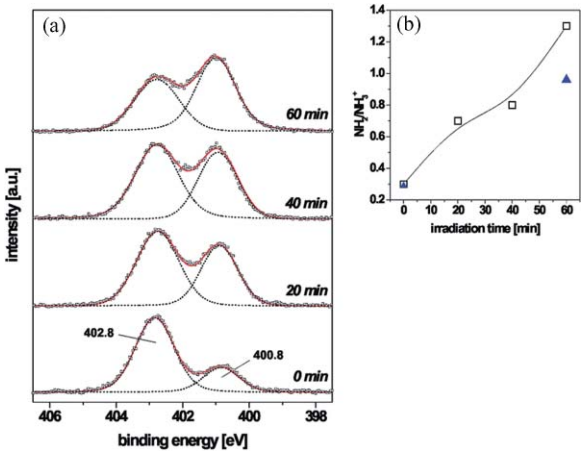

FIG. 3. (a) Time evolution of N1s photoemission spectrum of G6W10 during continuous exposure to x-rays; spectra at the beginning of irradiation (0 min) and after 20, 40, and 60 min are presented. The dots are the measured data points, and the dashed lines are the components determined by the fitting procedure. The solid lines through the data points are the results of the fitting. (b) NH_2/NH_3^+ integrated intensity ratio for G6W10 (open symbols) and for G6W60 (filled symbols) as a function of irradiation time.

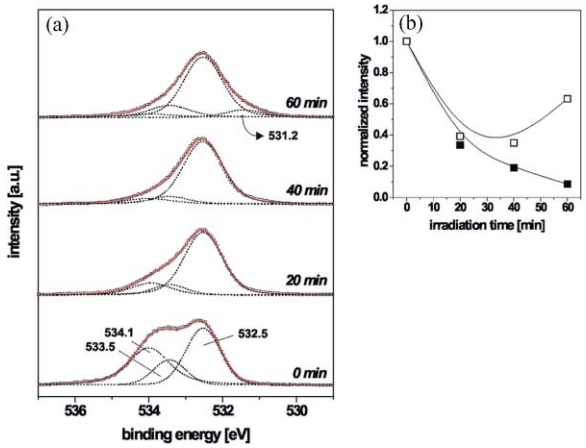

FIG. 4. (a) Time evolution of O1s photoemission spectrum of G6W10 during continuous exposure to x-rays; spectra at the beginning of irradiation (0 min) and after 20, 40, and 60 min are presented. The dots are the measured data points, and the dashed lines are the components determined by the fitting procedure. The solid lines through the data points are the results of the fitting. (b) Integrated peak intensities of H_2O (filled symbols) and OH (open symbols) components as a function of irradiation time.

continuously increase in intensity upon irradiation. In the spectrum after 20 min of irradiation a signal at 292.5 eV is also observed. In our recent study of the chemical evolution of a pure 150 Å thick glycine film irradiated with an Al K_α x-ray source (1486.6 eV), the same feature was detected, and it was assigned to CO_2 species resulting from glycine decarboxylation caused by α-C–COOH bond scission.[20] It was also demonstrated that the CO_2 molecules stay on the 110 K cold substrate, entrapped in the organic overlayer. Interestingly, in the present examination, the component at 292.5 eV disappears after prolonged time of illumination (see Fig. 2(a)). A possible reason for that will be discussed below.

The evolution of the N1s spectral region of the G6W10 film upon x-ray irradiation is presented in Fig. 3(a). The spectrum of the pristine film shows two spectral components at 400.8 eV and 402.8 eV BEs. The high BE peak is due to the protonated amino group ($-NH_3^+$), which is characteristic for the zwitterionic form of glycine in the condensed phase. The low BE component in the N1s spectrum is always present in the XPS spectra of amino acids in solid state, and it is mainly due to the NH_2 species formed by the deamination of the irradiated molecules.[15,20,27] Furthermore, the enrichment of the exposed film with additional NH_2 containing fragments cannot be ruled out. As one can see in Fig. 3(b), the integrated intensities of the two N1s components change significantly in opposite direction; the increase of the NH_2 component as a function of irradiation time demonstrates the continuous deamination of the glycine part of the G6W10 film.

Figure 4(a) shows the effect of irradiation on the O1s photoemission structure of G6W10. The spectrum of the starting film shows an asymmetric peak, which can be deconvoluted into three components at 532.5 eV, 533.5 eV, and 534.1 eV. The components at 532.5 eV and 534.1 eV are ascribed to the O1s emission of the glycine carboxyl group and of H_2O, respectively. The component at 533.5 eV is due to the hydroxyl oxygens of nondeprotonated COOH groups in some neutral glycine molecules (NH_2CH_2COOH) in the film and, probably, to OH groups from water photolysis. Amino acid molecules in their neutral form can exist as minority species in thick condensed glycine films. This is due to the fact that glycine exists in the neutral form in its gas state and upon adsorption at low temperatures the vapors cannot be completely transformed into the zwitterionic form.[35] As apparent in Fig. 4(a), the main effect of 20 min irradiation can be associated with the strong decrease of the water intensity (see also Fig. 4(b)). Furthermore, in the spectrum recorded after 40 min of irradiation a new peak centered at 531.2 eV appears. The BE position of the latter is in good agreement with that observed for the bare AlO_x/NiAl(110) surface.[25] Both, the continuous decrease of water and the increase of the substrate oxide signal, strongly suggest that a reduction of the G6W10 film thickness as a result of x-ray irradiation takes place. According to the O1s data presented in Fig. 4(a), this reduction is primarily due to the loss of H_2O from the G6W10 film. Evidently, this interpretation agrees well with the observed disappearance of the CO_2 photoemission signal in the C1s spectrum presented in Fig. 2(a). The radiation-produced CO_2 molecules are captured into the 20 min x-ray processed G6W10 film, but they desorb after prolonged times of irradiation, since a thinner overlayer is developed.

In order to gain a better understanding of the physicochemical changes in the G6W10 film upon x-ray illumination, the evolution of the valence band photoemission spectrum of the film after 60 min of irradiation was also examined. The spectrum of the as-grown film is presented in Fig. 5. It contains the emission signals for both glycine and water. The presence of glycine in zwitterionic form is manifested in the bands centered at 6.5, 10.6, and 13.3 eV below E_F.[36] The features at 7, 8.5, and at 13 eV below E_F are attributed to the emission from the three highest occupied molecular orbitals (MOs) of water.[13] The first peak corresponds to emission from the non-bonding oxygen lone pair $1b_1$ MO of water, the second feature is due to the partly

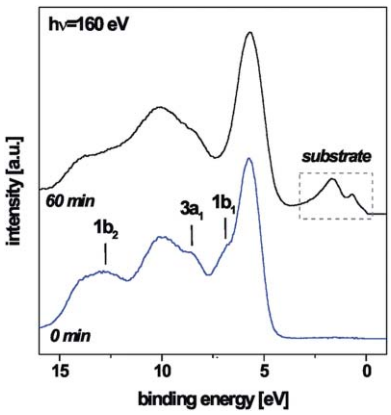

FIG. 5. Valence band photoemission spectra obtained from the as-grown G6W10 and from the same film after 60 min of x-ray irradiation.

bonding and partly non-bonding $3a_1$ MO, and the last one at 13 eV is caused by the bonding $1b_2$ MO. As one can see in Fig. 5, after 60 min of x-ray exposure the water signals are reduced. Furthermore, new features at 0–3 eV below E_F have developed. The latter emission is due to the Al(sp)–Ni(d) band from the NiAl(110) substrate.[37] The thickness of the alumina layer is ~5 Å (Ref. 23) and therefore the x-rays easily probe the NiAl(110) crystal substrate. The spectral evolution presented in Fig. 5 corroborates the core level photoemission results. Again, a clear loss of the water fingerprint is observed. The decrease of the G6W10 film thickness is demonstrated by the appearance of the substrate photoemission. Finally, the detailed analysis of the valence band spectra presented in Fig. 5 shows that the width of most intense glycine band centered at 6.5 eV becomes somewhat larger after 60 min of x-ray processing. Most probably this is due to a contribution from molecular fragments formed as a result of photodecomposition of the G6W10 film.

C. Radiation-induced effects in the G6W60 film

The changes in the C1s and N1s spectral regions of the G6W60 film after 60 min of irradiation are displayed in Figs. 6(a) and 6(b). Apparently, the spectral lineshapes are very similar to those of the G6W10 film after the same time of beam illumination. Nevertheless, the deconvolution procedure reveals some important differences. First, as it is shown in Fig. 6(a), the C1s spectrum of the irradiated G6W60 sample does not show photoemission at 284.6 eV as the spectrum from G6W10. Second, the component at ~292 eV, which is due to the CO_2 decomposition-created molecules, is still present in the spectrum after 60 min of continuous irradiation in contrast to the G6W10 sample (see Fig. 2(a)). Most probably, the lack of the component at ~285 eV is explained with the reduced rate of beam-induced disintegration of glycine in G6W60 and/or with the different pathways of glycine photodecomposition. The latter is associated with the influence of the substrate, which can play a role in the radiation-induced electronic transitions in the adsorbates in the case of the thinner G6W10 sample. The presence of the CO_2 signal is due to the morphology of the G6W60, i.e., the mixed layers are thick enough to hold the CO_2 species even after prolonged times of irradiation. This explanation is confirmed in the C1s spectrum of the 60 min irradiated G6W60 film recorded after warming up the sample to 273 K (top spectrum of Fig. 6(a)). According to the TPD data in Fig. 1, at this temperature water fully desorbs, while glycine molecules stay on the substrate. As one can see, the CO_2 signal in the C1s spectrum disappears along with desorption of the ice layers. There is also intensity increase of the component at 285.9 eV (hydrocarbon fragments) in the spectrum of the heated sample. The latter might be due to some temperature-driven processes in the illuminated sample or due to a re-arrangement of the species inside the film during water desorption. Finally, the change of the integrated intensity ratio of the zwitterionic glycine components CH_2NH_2 and COO^- after 60 min of x-ray processing is displayed in Fig. 2(b). As one can see, there is an increase of the ratio due to the beam-induced reduction of the carboxyl carbon fraction in the film. Furthermore, the increase of the CH_2NH_2/COO^- ratio for the G6W10 film is 30% higher than the increase obtained for G6W60 structure after 60 min of x-ray irradiation.

The alteration of N1s photoemission spectrum of G6W60 after 60 min of irradiation is presented in Fig. 6(b). Similar to the spectral changes observed for G6W10, a significant increase of the NH_2 and a decrease of the NH_3 component are detected. The change of the NH_2/NH_3^+ spectral components ratio after 60 min of irradiation is shown in Fig. 3(b). It appears that the change of this ratio for the G6W10 film is 33% higher than the increase achieved for G6W60. Thus, the rate of deamination and decarboxylation (see above) processes of glycine in the G6W10 film is about 30% higher than that for glycine in G6W60.

Not surprisingly, the dominating feature at 534.1 eV in the O1s spectrum of the starting G6W60 film is due to the water, as shown in Fig. 6(c). Contrary to the O1s spectral region evolution of G6W10, the water signal appears as the major component in the spectrum of the 60 min x-ray processed G6W60 sample. The photoemission data presented in Fig. 6(c) also show a suppression of the O1s signal from glycine zwitterions at 532.5 eV in the irradiated film. The latter observation is consistent with the beam-induced decomposition of glycine molecules which includes decarboxylation and leads to a decrease of the COO^- photoemission at 532.5 eV. Furthermore, the O1s component at 533.5 eV grows somewhat in intensity after 60 min of irradiation, thus indicating the enrichment of the G6W60 surface with OH groups.

In addition, the effect of 610 eV irradiation on the G6W60 film was examined using valence band photoemission spectroscopy. The spectrum of the pristine film is compared with the spectrum of the 60 min irradiated film in Fig. 6(d). Both spectra show the characteristic $1b_1$, $3a_1$, and $1b_2$ MOs of water. As one can see, no big changes due to the x-ray illumination are observed. Glycine photoemission is greatly suppressed by the water signal and only the most intense feature of glycine at 6.5 eV below E_F is present as a shoulder of the $1b_1$ peak (see the arrow). This signal is further suppressed after 60 min of irradiation due to the beam-induced chemical changes of the amino acid molecules. Also, the width of the $1b_1$ water band becomes larger as a result of the x-ray processing. Here we would like to comment on the

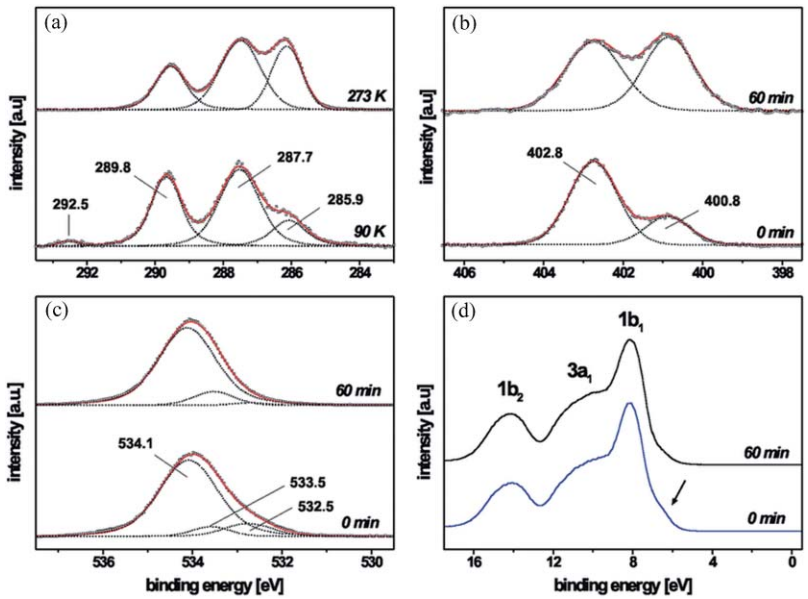

FIG. 6. (a) C1s photoemission spectrum of 60 min x-ray irradiated G6W60 recorded at 90 K and after warming the film up to 273 K. (b) N1s photoemission spectra of G6W60 recorded at the beginning of irradiation (0 min) and after 60 min of x-ray irradiation. (c) O1s photoemission spectra of G6W60 recorded at the beginning of irradiation (0 min) and after 60 min of x-ray irradiation. (d) Valence band photoemission spectra of G6W60 recorded at the beginning of irradiation (0 min) and after 60 min of x-ray irradiation.

photoemission from OH groups in the valence band spectra presented in Figs. 5 and 6. Since the contribution from hydroxyls is always present in the O1s core level spectra of both films and, furthermore, according to the deconvolution analysis the OH peaks grow in intensity as a result of x-ray processing (see also Fig. 4(b)), one can expect that OH bands will also appear in the valence band spectra. The OH spectral features usually emerge at 7.2 eV and 11.3 eV and can be assigned to the 1π and 3σ levels of OH species.[13] Most probably, these signals are masked by the intense features of glycine and water in the valence band spectra in Figs. 5 and 6. Eventually, the 1π band may contribute to the width change of the intense glycine band centered at 6.5 eV and of the $1b_1$ water band in the valence band spectra of the x-ray processed G6W10 and G6W60, respectively.

IV. DISCUSSION

The photoemission data presented above clearly demonstrate that glycine molecules in the mixed glycine-water ice films are very sensitive to soft x-ray irradiation. Even the first photoemission spectrum taken from the as-grown glycine-water ice films already shows beam-induced damages. On the basis of the deconvolution analysis of the core-level spectra, we summarize the major radiation-induced effects of glycine as follows: First, a removal of CO_2 from glycine molecules as a result of α-C–COOH bond scission is detected. Second, the increasing NH_2/NH_3^+ ratio in the N1s photoemission spectra upon irradiation can be associated with the direct detachment of the nonprotonated amino group from the amino acid molecule due to C–N bond scission. Finally, in the C1s spectral region some fragments with carbon atoms without strong electronegative substituents (C–C and C–H) are recognized. The release of CO_2 is in accord with the systematic quantum chemical calculations performed by Lattelais *et al.*[21] very recently. These authors have shown that under photon irradiation glycine zwitterions $NH_3^+CH_2COO^-$ convert to glycine cations $(NH_3^+CH_2COO^-)^+$ which break spontaneously releasing CO_2. Furthermore, the changes in the C1s and N1s spectral regions are very similar to the changes of XPS spectra recorded during continuous illumination of pure glycine films with an Al K_α x-ray source (1486.6 eV) for over 360 min.[20] Reasonably, due to the intense synchrotron radiation, the spectral changes reported here are much more pronounced. On the basis of the change of the integrated intensity ratios of the C1s and N1s components (CH_2NH_2/COO^- and NH_2/NH_3^+, respectively) in the photoemission spectra of the films, we can conclude that the rate of photodecomposition of glycine in G6W10 is about 30% higher than for glycine in the thicker film (G6W60).

The evolution of the O1s spectral regions of the samples during irradiation gives us information of the changes in the water ice part of the layers. As shown in Fig. 4(a), in the case of G6W10 the photoemission signal from water is greatly suppressed and the film became thinner as a result of the interaction with the x-ray beam. Presently, it is well known that condensed H_2O can dissociate upon nonthermal activation by x-ray photons and the production of different radicals and molecules, such as H, H_2, O, OH, H_2O_2, HO_2, and O_2, have been reported.[13,38,39] In our O1s spectra (see Figs. 4(a) and 6(c)) the OH spectral component is always present, but we cannot unambiguously ascribe this signal to a water fragment since glycine neutral molecules (NH_2CH_2COOH) and/or by-products also contain OH groups. We presume that the disappearance of the water molecules from the surface of G6W10 during the x-ray

photoprocessing is due to the following processes. First, fragmentation of H_2O and subsequent desorption of the photoproduced species. Second, we cannot preclude the possibility of desorption of H_2O into the gas phase due to heating of the samples from the intense x-ray beam. During the entire experiment, we did not observe any changes of the crystal temperatures, but nevertheless, a local rise of the temperature cannot be fully excluded. Finally, disordering in the layers and re-arrangement of the molecular fragments in the bulk of the samples as a result of x-ray illumination may also take place. The latter can open cracks in the films and the substrate photoemission signal may appear in the spectra as shown in our results. Additionally, the bare substrate can influence the process of photodecomposition since the photon excited states in the film are expected to be more rapidly quenched in the vicinity of the substrate surface.

In summary, the mechanism of x-ray interaction with the glycine-water ice structures is complex, consisting of numerous steps. Our photoemission experiments demonstrate that the structure of the mixed layers employed in the present study influences the rate of x-ray induced degradation of glycine molecules. In the thinner G6W10 film where the glycine/water molecules are homogeneously intermixed, the H_2O molecules strongly suffer from the x-ray beam and cannot protect the amino acid from photodecomposition. In the thicker G6W60 film the glycine molecules are located near to the surface region but due to the water excess the degree of glycine disintegration is smaller. Hence, an enhanced photostability of amino acids in mixed systems with water ice can be observed, if the organic molecules are deeply hidden into the water matrix. Certainly and trivially, water ice can provide a real protection to glycine when the amino acid is buried at depths higher than the x-ray photon penetration.

Our photoemission results do not provide a direct evidence for artifacts formed as a result of the interaction between glycine and the species released by H_2O radiolysis in the x-ray processed films. This is in accord with the results obtained by Parent *et al.*[40] in the course of 530 eV synchrotron irradiation of mixed glycine-ice films at 30 K. Later the authors concluded that water plays no role in the destruction of glycine. Nevertheless, secondary reactions might occur in the films initiated by the resulting free radicals and fragments from H_2O and glycine. Cornelson *et al.*[41] reported that soft x-ray bombardment of adsorbed CO_2 leads to a direct photolysis of the molecules producing CO and unidentified O products, possibly atomic O. This effect may play a role in thicker glycine-water ice films where CO_2 originating from decarboxylation of the amino acid accumulates on the surface of the samples. Furthermore, the development of active chemisorption sites on the films as a result of the constant x-ray illumination may cause sticking of the residual hydrogen from the vacuum environment on the surface. The latter can react with other molecules and fragments in the sample producing new species. Further studies with additional analytical techniques are needed in order to understand the full spectrum of photochemical events during x-ray irradiation of mixed amino acid-water ice layers.

ACKNOWLEDGMENTS

This work has been supported by the Austrian Science Funds (FWF).

[1] M. P. Bernstein, S. A. Sandford, L. J. Allamandola, J. S. Gillette, S. J. Clemett, and R. N. Zare, Science **283**, 1135 (1999).
[2] C. C. Perry, G. M. Wolfe, A. J. Wagner, J. Torres, N. S. Faradzhev, T. E. Madey, and D. H. Fairbrother, J. Phys. Chem. B **107**, 12740 (2003).
[3] L. Krim, J. Lasne, C. Laffon, and Ph. Parent, J. Phys. Chem. A **113**, 8979 (2009).
[4] C. Laffon, J. Lasne, F. Bournel, K. Schulte, S. Lacombe, and Ph. Parent, Phys. Chem. Chem. Phys. **12**, 10865 (2010).
[5] C. R. Arumainayagam, H.-L. Lee, R. B. Nelson, D. R. Haines, and R. P. Gunawardane, Surf. Sci. Rep. **65**, 1 (2010).
[6] A. G. G. M. Tielens and W. Hagen, Astron. Astrophys. **114**, 245 (1982) http://adsabs.harvard.edu/full/1982A%26A...114..245T.
[7] P. Ehrenfreund and S. B. Charnley, Annu. Rev. Astron. Astrophys. **38**, 427 (2000).
[8] F. Dominé and P. B. Shepson, Science **297**, 1506 (2002).
[9] S. Lacombe and C. L. Sech, Surf. Sci. **603**, 1953 (2009).
[10] J. E. Elsila, J. P. Dworkin, M. P. Bernstein, M. P. Martin, and S. A. Sandford, Astrophys. J. **660**, 911 (2007).
[11] J. E. Elsila, D. P. Glavin, and J. P. Dworkin, Meteorit. Planet. Sci. **44**, 1323 (2009).
[12] D. P. Glavin, A. D. Aubrey, M. P. Callahan, J. P. Dworkin, J. E. Elsila, E. T. Parker, J. L. Bada, P. Jenniskens, and M. H. Shadad, Meteorit. Planet. Sci. **45**, 1695 (2010).
[13] M. A. Henderson, Surf. Sci. Rep. **46**, 1 (2002).
[14] M. J. Bozack, Y. Zhou, and S. D. Worley, J. Chem. Phys. **100**, 8392 (1994).
[15] Y. Zubavichus, O. Fuchs, L. Weinhardt, C. Heske, E. Umbach, J. D. Denlinger, and M. Grunze, Radiat. Res. **161**, 346 (2004).
[16] Y. Zubavichus, M. Zharnikov, A. Shaporenko, O. Fuchs, L. Weinhardt, C. Heske, E. Umbach, J. D. Denlinger, and M. Grunze, J. Phys. Chem. A **108**, 4557 (2004).
[17] R. G. Wilks, J. B. MacNaughton, H.-B. Kraatz, T. Regier, R. I. R. Blyth, and A. Moewes, J. Phys. Chem. A **113**, 5360 (2009).
[18] F. Kaneko, M. Tanaka, S. Narita, T. Kitada, T. Matsui, K. Nakagawa, A. Agui, K. Fujii, and A. Yokoya, J. Electron Spectrosc. Relat. Phenom. **144–147**, 291 (2005).
[19] A. Sanderud and E. Sagstuen, J. Phys. Chem. B **102**, 9353 (1998).
[20] G. Tzvetkov and F. P. Netzer, J. Electron Spectrosc. Relat. Phenom. **182**, 41 (2010).
[21] M. Lattelais, O. Risset, J. Pilmé, F. Pauzat, Y. Ellinger, F. Sirotti, M. Silly, Ph. Parent, and C. Laffon, Int. J. Quantum Chem. **111**, 1163 (2011).
[22] G. Tzvetkov, M. G. Ramsey, and F. P. Netzer, J. Chem. Phys. **122**, 114712 (2005).
[23] R. M. Jaeger, H. Kuhlenbeck, H.-J. Freund, M. Wuttig, W. Hoffmann, R. Franchy, and H. Ibach, Surf. Sci. **259**, 235 (1991).
[24] G. Kresse, M. Schmid, E. Napetschnig, M. Shishkin, L. Köhler, and P. Varga, Science **308**, 1440 (2005).
[25] G. Tzvetkov, Y. Zubavichus, G. Koller, Th. Schmidt, C. Heske, E. Umbach, M. Grunze, M. G. Ramsey, and F. P. Netzer, Surf. Sci. **543**, 131 (2003).
[26] G. Tzvetkov, M. G. Ramsey, and F. P. Netzer, Chem. Phys. Lett. **397**, 392 (2004).
[27] G. Tzvetkov, G. Koller, Y. Zubavichus, M. B. Casu, O. Fuchs, C. Heske, E. Umbach, M. Grunze, M. G. Ramsey, and F. P. Netzer, Langmuir **20**, 10551 (2004).
[28] E. Mayer and R. Pletzer, Nature (London) **319**, 298 (1986).
[29] R. Pletzer and E. Mayer, J. Chem. Phys. **90**, 5207 (1989).
[30] R. S. Smith, C. Huang, E. K. L. Wong, and B. D. Kay, Surf. Sci. **367**, L13 (1996).
[31] M. S. Westley, G. A. Baratta, and R. A. Baragiola, J. Chem. Phys. **108**, 3321 (1998).
[32] K. P. Stevenson, G. A. Kimmel, Z. Dohnálek, R. S. Smith, and B. D. Kay, Science **283**, 1505 (1999).
[33] R. S. Smith and B. D. Kay, Nature (London) **398**, 788 (1999).
[34] D. T. Clark, J. Peeling, and L. Colling, Biochim. Biophys. Acta **453**, 453 (1976).

[35]P. Löfgren, A. Krozer, J. Lausmaa, and B. Kasemo, Surf. Sci. **370**, 277 (1997).
[36]K. H. Ernst and K. Christmann, Surf. Sci. **224**, 277 (1989).
[37]G. Tzvetkov, M. G. Ramsey, and F. P. Netzer, Surf. Sci. **526**, 383 (2003).
[38]C. Laffon, S. Lacombe, F. Bournel, and Ph. Parent, J. Chem. Phys. **125**, 204714 (2006).
[39]R. A. Baragiola, M. Famá, M. J. Loeffler, U. Raut, and J. Shi, Nucl. Instr. Meth. B **266**, 3057 (2008).
[40]Ph. Parent, C. Laffon, F. Bournel, J. Lasne, and S. Lacombe, J. Phys.: Conf. Ser. **261**, 012008 (2011).
[41]D. M. Cornelson, T. R. Dillingham, S. C. Tegler, K. Galle, G. A. Miller, and B. L. Lutz, Astrophys. J. **505**, 443 (1998).